Transactions of NAMP 22, (2025) 67-84

Transactions of
The Nigerian Association of
Mathematical Physics
Journal homepage: https://nampjournals.org.ng

PRESCRIBED SURFACE TEMPERATURE AND PRESCRIBED HEAT FLUX ANALYSIS OF JEFFREY FERROFLUID FLOW OVER VERTICAL STRETCHABLE PLATE WITH MAGNETIC DIPOLE EFFECT

*** [1] Iyoko, M. O., [2] Olajuwon, B. I., [3] Fagbemiro, O. and [4] Raji, M. T.**
[1,2,3,4]Federal University of Agriculture, Abeokuta, Nigeria

ARTICLE INFO

Article history:
Received 4/3/2025
Revised 30/6/2025
Accepted 30/6/2025
Available online 17/7/2025

Keywords:
Jeffrey fluid,
Vertical stretching sheet,
Prescribed surface temperature,
Magnetic dipole,
Suction/injection

ABSTRACT

The flow of Jeffery ferrofluid over a vertical stretching sheet in the presence of magnetic dipole and suction/injection was considered. Similarity transformations transformed the governing equations into nonlinear ordinary differential equations which were solved using the Chebyshev spectral collocation method. Effects of the existing parameters on the flow and heat transfer were presented in graphs and tables. Results obtained were compared with those in the literature and showed good agreement. Grashof number increased fluid velocity and reduced fluid temperature, it increased Nusselt number and decreased skin friction. Magnetic dipole reduced velocity and increased temperature. The Suction parameter ($S > 0$ *) reduced Nusselt number and increased skin friction. These findings are useful in industrial applications such as the cooling of voice coils in loudspeakers and magnetic hyperthermia.*

1. INTRODUCTION

The knowledge of boundary layer flow and heat transfer past a stretching sheet has applications in various industrial and engineering processes like manufacturing of paper and polythene, stretching of plasma film, casting out of polymer, cooling of stretchable sheets, crystals culturing, wire stretching and fibre engineering, etc. As a result, examination of flow of fluids past stretching sheets has gained the interest of many. Zeeshan and Majeed [1] opined that the study of heat transfer is relevant as findings from the analysis help for easy control of the rate of cooling to arrive at the desired quality of the end products. A study of boundary layer flow past a continuously stirring flat plate was carried out by Sakiadis [2]. Crane [3] found a fundamental closed-form solution for a 2-D boundary layer flow past a straight elastic sheet whose velocity is proportional to the distance from the origin. A further study by Gupta and Gupta [4] incorporated suction with heat and mass transfer.

*Corresponding author: IYOKO, M. O.
E-mail address: ojbiyoko@gmail.com
https://doi.org/10.60787/tnamp.v22.554

The Jeffery fluid as a non-Newtonian fluid has linear model equations and uses time derivatives unlike convected derivatives used in fluid models such as the Maxwell fluid (Dalir [5]). The property of relaxation and retardation times existing in fluids such as emulsions, polymer solutions, and slurries is emphasized by Jeffery fluid model. Hayat et al. [6] studied a magneto hydrodynamic stagnation point flow of Jeffery fluid whose viscosity is dissipated as it flows over a stretching plate in the presence of joule heating. Sandeep et al. [7] carried out the analysis of the effect of chemical reaction and generated magnetic force on the stagnation point flow of MHD Jeffrey Nano fluid past a stretching plate. The flow of Jeffery fluid through a permeable conduit which a magnetic field is acting across was studied by Hayat et al. [8]. Narayana et al. [9] examined a micropolar ferromagnetic fluid flow over a stretching plate experiencing a magnetic field.

The flow of non-Newtonial fluids over vertically inclined stretching sheets has many applications in the industry and has been treated by many research as can be found in the literature. Ahmad and Ishak [10] studied the magneto hydrodynamic Jeffery fluid past a vertical stretching sheet in a permeable enveloping substance and discovered there is reduction in the heat transfer as magnetic parameter increases while Prandtl number causes the heat transfer to increase; also, the magnitude of the skin friction is decreased by the flow of the Jeffery fluid and it brought about a small increase in the heat transfer at the surface. Titus and Abraham [11] worked on ferromagnetic liquid flow over a stretching plate that is positioned in such a way that gravity supports its stretching and concluded that the ferromagnetic relation parameter reduces velocity, whereas it temperature to increase. Grashof and Prandtl numbers increase the flow and reduce heat transfer so they must be minimal for effective cooling. Iyoko and Olajuwon [12] worked on an MHD flow of a third-grade fluid with joule heating and Reynolds' model viscosity using the differential transform method, from which it was realized that the magnetic force decreases fluid temperature as well as velocity and increment in Joule heating bring about a reduction in fluid temperature at the middle of the pipe. Akinbo and Olajuwon [13] looked at the impact of thermal-diffusion and convective boundary conditions on Walters' B fluid flowing past a vertical stretching plate. Akinbo and Olajuwon [14] analyzed thermal-diffusion and radiation interaction on the stagnation-point flow of Walters' B fluid over a vertically inclined stretching plate. The impact of viscous dissipation, thermal diffusion and thermal radiation on magneto hydrodynamic fluid flow over an exponential plate was considered by Akinbo and Olajuwon [15] and it was found that at low Prandtl numbers, there is strong thermal conductivity in the fluid.

Andersson and Valnes [16] gave a detailed analysis of a ferrofluid that is heated as it flows past a stretching plate where magnetic dipole is present. Some applications of ferrofluids includes, inclinometers, affinity chromatography, loudspeakers, crack detection in metals, ink jet printing, accelerometers, etc. (Bailey [17]). Zeeshan and Majeed [1] considered Jeffery fluid as a ferrofluid and worked on its heat transfer and flow past a stretching plate with influence of magnetic dipole and suction/injection; and found that the magnetic dipole increases temperature and decreases the fluid velocity. Also, the suction/injection parameter brings about decrement in the thickness of thermal boundary layer. Iyoko and Olajuwon [18] examined the influence of thermal radiation, suction/injection and magnetic dipole on Jeffery fluid flowing past a stretching plate; which was an extension of the work by Zeeshan and Majeed [1]. The model equation was solved using Chebyshev Spectral Collocation Method and it was discovered that thermal radiation increases temperature for the prescribed surface temperature (PST) as well as the prescribed heat flux (PHF) process. Also, there is an increment in temperature and a reduction in fluid velocity as magnetic dipole increases.

Previous research by Zeeshan and Majeed [1] and Iyoko and Olajuwon [18] only considered a flow on a horizontal stretching sheet without finding out the behavior of the fluid when the sheet

is inclined. Motivated by the work of Iyoko et al. [19] which studied Jeffrey fluid flow past an inclined stretchable sheet with magnetic dipole and suction/injection, this work incorporates gravitation acceleration into the momentum equation of Zeeshan and Majeed [1] to consider Jeffery fluid as a ferrofluid flowing past a vertical stretchable plate where magnetic dipole and suction/injection is present. The method of Chebyshev Spectral Collocation shall be used to find the solution to the problem. The various thermos-physical parameters shall be varied and temperature and velocity profiles presented with detailed explanations.

Nomenclature

(x, y)	Coordinates along and normal to the sheet (m)	θ	Dimensionless temperature
c	Stretching rate (s^{-1})	μ_0	Magnetic permeability
k	Thermal conductivity $(Wm^{-1}K^{-1})$		
a	Distance	***Greek symbols***	
H	Magnetic field (A/m)	μ	Dynamic viscosity $(Ns\ m^{-1})$
C_f	Skin friction coefficient	$\lambda_1,\ \lambda_2$	Material parameters of Jeffery fluid
f	Dimensionless stream function	α_1	Dimensionless distance
(u, v)	Velocity components $(m\ s^{-1})$	ν	Kinematic viscosity
κ	Extra stress tensor	β	Ferromagnetic interaction parameter
g	Gravitational acceleration	β_T	Thermal expansion
c_p	Specific heat at constant pressure $(J\ kg^{-1}\ K^{-1})$	γ_1	Deborah number
v_w	Suction/injection velocity		
Re_x	Local Reynolds number	ρ	Density $(kg\ m^{-3})$
Gr	Grashof number	(η, ξ)	Dimensionless coordinates
Pr	Prandtl number	τ	Cauchy stress tensor
Nu_x	Local Nusselt number	γ	Magnetic field strength (A/m)
K^*	Pyromagnetic coefficient	ε	Dimensionless curie temperature
S	Suction/injection parameter	ϕ	Magnetic potential
M	Magnetization (A/m)	λ	Viscous dissipation parameter
T	Temperature (K)	ψ	Stream function $(m^2\ s^{-1})$
A_1	Rivlin-Ericksen tensor		
T_c	Curie temperature (K)		

2. METHODS

2.1. Magnetic dipole

The permanent magnetic scalar potential (φ) of a dipole field usually affects the flow of a magnetic fluid. We write φ as

$$\varphi = \frac{\gamma}{2\pi}\left(\frac{x}{x^2 + (y+a)^2}\right) \tag{1}$$

where γ is the potency of the magnetic field. The intensity of the magnetic field along the x axis is H_x, while that along the y axis is H_y. They are written as:

$$H_x = -\frac{\partial \varphi}{\partial x} = \frac{\gamma}{2\pi}\left(\frac{x^2-(y+a)^2}{\left(x^2+(y+a)^2\right)^2}\right) \tag{2}$$

$$H_y = -\frac{\partial \varphi}{\partial y} = \frac{\gamma}{2\pi}\left(\frac{2x(y+a)}{\left(x^2+(y+a)^2\right)^2}\right) \tag{3}$$

The resulting magnitude H of these intensities gives

$$H = \left[\left(\frac{\partial \varphi}{\partial x}\right)^2 + \left(\frac{\partial \varphi}{\partial y}\right)^2\right]^{\frac{1}{2}} \tag{4}$$

$$\frac{\partial H}{\partial x} = -\frac{\gamma}{2\pi}\left(\frac{2x}{(y+a)^4}\right) \tag{5}$$

$$\frac{\partial H}{\partial y} = \frac{\gamma}{2\pi}\left(\frac{-2}{(y+a)^3} + \frac{4x^2}{(y+a)^5}\right) \tag{6}$$

Anderson and Valnes [16] stated that the variation of magnetization M is considered as a linear relationship of temperature and written as

$$M = K^*(T_c - T) \tag{7}$$

Such that K^* is the pyromagnetic factor, while T_c is the Curie temperature; although, for ferrohydrodynamic influence to take place, the following must apply:

(a) fluid temperature T is different from T_c, and

(b) the magnetic field from outside is not homogeneous. Immediately the ferromagnetic fluid approaches Curie temperature, magnetization ceases. Characteristics for physical significance is very essential, since Curie's temperature is very high, for example, it is 1043 K for iron.

2.2 Analysis of the flow

A Jeffrey fluid flowing in two dimensions past a vertical stretchable plate influenced by magnetic dipole is examined. Electricity conduction property is inexistent in the fluid. The vertical axis is considered the x-axis along which we have the stretching plate and its velocity is $u_w = cx$, while the horizontal axis is the y-axis. Figure 1 gives a diagrammatic representation. At a distance ''a" from the stretchable sheet and mid-point of the horizontal axis, a magnetic dipole is situated. The magnetic field is along the positive x-axis due to the magnetic dipole and the intensity of the magnetic field continue to increase until the ferrofluid gets steeper. The Curie temperature T_c is assumedly more than the temperature on the plate T_w. On the other hand, $T_\infty = T_c$ is the temperature of the ambient fluid which magnetizes only when it gets to the region close to the plate. Because the stretching sheet is vertical, the force of gravity (g) acts downward in the positive x-direction.

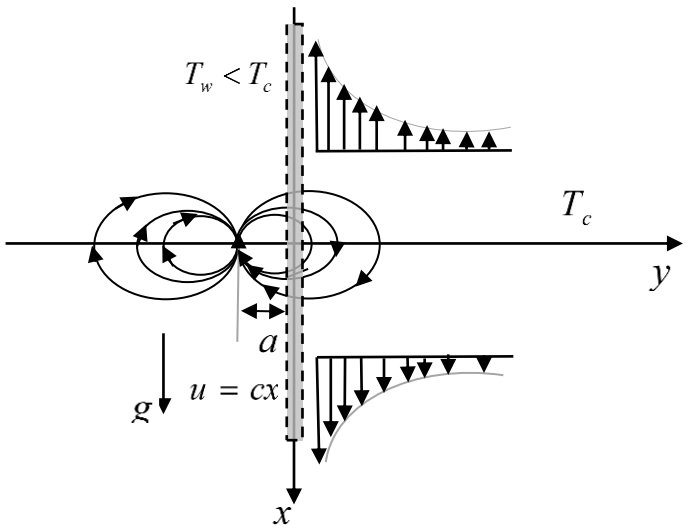

Figure 1: Vertically inclined plate with magnetic dipole influencing the fluid flow

Nadeem and Akbar [20] presents the Jeffery fluid equations as:

$$\tau = -pI + \kappa \tag{8}$$

$$\kappa = \frac{\mu}{1+\lambda_2}\left[A_1 + \lambda_1\left(\frac{\partial A_1}{\partial t} + \mathbf{V}\cdot\nabla A_1\right)\right] \tag{9}$$

A_1, the Rivlin-Ericksen tensor is given as

$$A_1 = (\nabla\mathbf{V}) + (\nabla\mathbf{V})^T \tag{10}$$

Incorporating gravitational acceleration and thermal expansion coefficient as can be found in Ahmad and Ishak [10] and using boundary layer approximations, the continuity and momentum equations of Jeffery fluid become

$$\frac{\partial u}{\partial x} + \frac{\partial v}{\partial y} = 0 \tag{11}$$

$$u\frac{\partial u}{\partial x} + v\frac{\partial u}{\partial y} = \frac{\mu_0}{\rho}M\frac{\partial H}{\partial x} + \frac{\nu}{1+\lambda_2}\left[\frac{\partial^2 u}{\partial y^2} + \lambda_1\left(u\frac{\partial^3 u}{\partial x\partial y^2} + v\frac{\partial^3 u}{\partial y^3} - \frac{\partial u}{\partial x}\frac{\partial^2 u}{\partial y^2} + \frac{\partial u}{\partial y}\frac{\partial^2 u}{\partial x\partial y}\right)\right] + g\beta_T(T_c - T) \tag{12}$$

All symbols are as defined in table 1 below.

The boundary conditions required for the velocity profile are

$$u = u_w = cx,\ c > 0 \qquad v = v_w, \qquad \text{at } y = 0$$

$$u \to 0, \qquad \frac{\partial u}{\partial y} \to 0, \qquad \text{as } y \to \infty \tag{13}$$

According to Andersson and Valnes [16] the transformations below can be used on equation (12)

$$\psi(\xi,\eta)=\left(\frac{\mu}{\rho}\right)\xi\cdot f(\eta),\qquad \xi=\sqrt{\frac{c\rho}{\mu}}x,\qquad \eta=\sqrt{\frac{c\rho}{\mu}}y \tag{14}$$

where ξ,η are dimensionless coordinates. The coordinates of velocity are

$$u=\frac{\partial\psi}{\partial y}=cx\cdot f'(\eta),\qquad v=-\frac{\partial\psi}{\partial x}=-\sqrt{c\nu}\cdot f(\eta) \tag{15}$$

substituting equation (15) into (12) and comparing coefficients of order ξ^2, leads to:

$$f''-(1+\lambda_2)\left(f'^2-ff''\right)+\gamma_1(1+\lambda_2)\left(f''^2-ff^{iv}\right)-(1+\lambda_2)\frac{2\beta\theta_1}{(\eta+\alpha_1)^4}+(1+\lambda_2)Gr\theta_1=0 \tag{16}$$

the non-dimensional BCs are:

$$f=S,\qquad f'=1,\qquad \text{at } \eta=0$$

$$f'\to 0,\qquad f''\to 0,\qquad \text{as } \eta\to\infty \tag{17}$$

$\gamma_1=\lambda_1 c$, $\beta=\frac{\gamma\rho}{2\pi\mu^2}\mu_0K^*(T_c-T_w)$, $Gr=\frac{g\beta_T(T_w-T_c)}{c^2x}$, $S=\frac{-v_w}{\sqrt{c\nu}}$; $S>0$ meaning suction while $S<0$ means injection.

2.3 Transfer of heat

The energy equation as in Zeeshan and Majeed [1] is written as

$$\rho c_p\left(u\frac{\partial T}{\partial x}+v\frac{\partial T}{\partial y}\right)+\mu_0T\frac{\partial M}{\partial T}\left(u\frac{\partial H}{\partial x}+v\frac{\partial H}{\partial y}\right)=k\frac{\partial^2T}{\partial y^2}+\mu\left(\frac{\partial u}{\partial y}\right)^2+2\mu\left(\frac{\partial v}{\partial y}\right)^2 \tag{18}$$

The thermal BCs necessary for solving equation (18) are

$$\left.\begin{aligned} T=T_w=T_c-A\left(\frac{x}{l}\right)^2 \quad & for\ PST\\ q_w=-k\frac{\partial T}{\partial y}=D\left(\frac{x}{l}\right)^2 \quad & for\ PHF\end{aligned}\right\}\quad at\quad y=0$$

$$T\to T_c,\quad as\quad y\to\infty \tag{19}$$

where A and D are positive constants and $l=\sqrt{\nu/c}$ is the characteristic length.

With the introduction of the non-dimensional variable $\theta(\xi,\eta)$

$$\theta(\xi,\eta) \equiv \frac{T_c - T}{T_c - T_w} = \theta_1(\eta) + \xi^2 \theta_2(\eta), \tag{20}$$

where

$$T_c - T_w = A\left(\frac{x}{l}\right)^2 \quad for \;\; PST, \quad T_c - T_w = \frac{D}{k}\left(\frac{x}{l}\right)^2 \sqrt{\frac{\nu}{c}} \quad for \quad PHF\,.$$

The non-dimensional energy equations are derived when we put similarity transformations (14) and equation (20) in (18) as

$$\theta_1'' + Pr\left(f\theta_1' - 2f'\theta_1\right) + \frac{2\lambda\beta(\theta_1 - \varepsilon)f}{(\eta + \alpha_1)^3} - 2\lambda f'^2 = 0, \tag{21}$$

$$\theta_2'' + Pr\left(4f\theta_2' - 2f'\theta_2\right) + \frac{2\lambda\beta\theta_2 f}{(\eta + \alpha_1)^3} - \lambda\beta(\theta_1 - \varepsilon)\left[\frac{2f'}{(\eta + \alpha_1)^4} + \frac{4f}{(\eta + \alpha_1)^5}\right] - \lambda f''^2 = 0, \tag{22}$$

where the viscous dissipation parameter is $\lambda = \frac{c\mu^2}{\rho k(T_c - T_w)}$, the Prandtl number is given as $Pr = \frac{\mu c_p}{k}$, the non-dimensional distance from the origin to the magnetic dipole is $\alpha_1 = \sqrt{\frac{c\rho}{\mu}}a$, and the non-dimensional Curie temperature ratio is $\varepsilon = \frac{T_c}{T_c - T_w}$.

the thermal BCs are

$$\left.\begin{array}{lll} \theta_1 = 1, & \theta_2 = 0 & for\;\; PST \\ \theta_1' = -1, & \theta_2' = -1, & for\;\; PHF \end{array}\right\} \qquad at \quad \eta = 0$$

$$\theta_1 \to 0, \qquad \theta_2 \to 0 \qquad as \quad \eta \to \infty \tag{23}$$

The relevant parameters in the industry are Nusselt number and Skin-friction coefficient, given by

$$Nu_x \equiv \frac{xq_w}{-k\left(T_c - T_w\right)^2}, \qquad C_{fx} \equiv \frac{-2\tau_w}{\rho(cx)^2}, \tag{24}$$

the surface heat flux is q_w, while the surface shear stress is τ_w, and they are written as

$$\tau_w = \mu\left(\frac{\partial u}{\partial y}\right)_{y=0}, \qquad q_w = -\left(\frac{\partial T}{\partial y}\right)_{y=0} \tag{25}$$

Utilizing equations (14) and (20) on (24) results in

$$\left.\begin{aligned} &C_f Re_x^{1/2} = -2f''(0), \\ &Nu_x / Re_x^{1/2} = -\left(1+\frac{4}{3}R_d\right)\left(\theta_1'(0)+\xi^2\theta_2'(0)\right) \quad PST \\ &Nu_x / Re_x^{1/2} = 1\Big/\left(1+\frac{4}{3}R_d\right)\left(\theta_1'(0)+\xi^2\theta_2'(0)\right) \quad PHF \end{aligned}\right\}, \tag{26}$$

$Re_x = \dfrac{\rho c x^2}{\mu}$ is the Reynolds number. The Grashof number Gr most definitely affects the flow.

$\theta^*(0) = \dfrac{\theta_1'(0)}{\theta_1'(0)\big|_{Gr=0}}$ is used in place of $-\theta' = -\left(\theta_1'(0)+\xi^2\theta_2'(0)\right)$, as it does not depend on the distance ξ.

2.4 Method of Solution

Equations (16) and (21) as well as (17) and (23) are solved using Chebyshev Spectral Collocation Method (CSCM). The velocity and temperature, $f(\eta)$ and $\theta(\eta)$ that are not known are gotten by summing the linearly independent vectors $T_n(\eta)$ (Akaje and Olajuwon [21]), that is;

$$f(\eta) = \sum_{n=0}^{N} a_n T_n(\eta) \tag{27}$$

$$\theta(\eta) = \sum_{n=0}^{N} b_n T_n(\eta) \tag{28}$$

This approach utilizes Chebyshev polynomials N bounded on $[-1, 1]$ which is written as

$$T_n(\eta) = \cos\left(N \cos^{-1}\bar{\eta}\right) \tag{29}$$

The Gauss-Lobatto set according to Pruett and Streett [22] and also Sobamowo et. al. [23] is:

$$\bar{\eta}_j = \cos\left(\frac{\pi j}{N}\right), \quad j = 0,1,2,\ldots,N \tag{30}$$

This set is utilized to make $[-1, 1]$ discrete and to mark Chebyshev nodes within.

a_n and b_n are to be determined. The basis function definition is made to represent the infinite interval $[0, \infty]$ using this conversion function:

$$\eta = \frac{2\vartheta}{\vartheta_\infty - 1} \tag{31}$$

ϑ_∞ represents the skirting region of the stretchable plate.

Putting equations (27-30) into (16) and (21), the residuals are obtained, so that a_n and b_n are found at the same time ensuring that the residuals are minimized over the entire region.

RESULTS

Using Mathematica to Implement Chebyshev Spectral Collocation Method (CSCM) for the problem (equations 16, 17, 21, and 23), while varying the thermos-physical properties. Utilizing $\beta = 0.2$, $\lambda = 0.01$, $\lambda_2 = 0.1$, $\gamma_1 = 0.2$, $S = 0.1$, $\Pr = 1.0$, $Gr = 1.0$, $\alpha_1 = 1.0$, and $\varepsilon = 2.0$ as constants.

Table 1: Comparing Nusselt number $-\theta_1'(0)$ when $\beta = \lambda = \lambda_2 = \gamma_1 = S = Gr = 0$.

Pr	Abel et al. [24]	Zeeshan and Majeed [1]	Current result
0.72	1.0885	1.088527	1.08852523
1	1.3333	1.333333	1.33333333
3	_	2.509725	2.5097266
10	4.7968	4.796873	4.7956998

Table 2: Skin friction coefficient $-f''(0)$, Nusselt number $-\theta_1'(0)$ with temperature $\theta_1(0)$ for distinct $\beta, \lambda, \lambda_2, \gamma_1, S$ and Pr when $Gr = 0$.

Pr	β	λ_2	γ_1	S	λ	Series solution of Zeeshan and Majeed [1]			CSCM result		
						$-f''(0)$	PST $-\theta_1'(0)$	PHF $\theta_1(0)$	$-f''(0)$	PST $-\theta_1'(0)$	PHF $\theta_1(0)$
1.0	0.2	0.1	0.2	0.1	0.01	1.0470	1.3958	0.7138	1.0523	1.3954	0.7142
2.0						1.0399	2.1184	0.4697	1.0000	2.0000	0.5000
3.0						1.0357	2.6848	0.3705	1.0000	2.5097	0.3985
3.0	2.0	0.1	0.2	0.1	0.01	1.3986	2.6458	0.3706	1.4411	2.6406	0.3710
	3.0					1.6042	2.6223	0.3705	2.3730	0.0908	2.3629
	4.0					1.8131	2.5973	0.3708	2.8094	0.1762	1.9841
3.0	0.2	0.1	0.2	0.1	0.01	1.0355	2.6848	0.3704	1.0397	2.6845	0.3707
		0.2				1.0814	2.6728	0.3722	1.0954	0.0526	18.9465
		0.3				1.1255	2.6613	0.3739	1.1402	0.0526	18.9963
3.0	0.2	0.1	0.1	0.1	0.01	1.0914	2.6710	0.3724	1.0962	2.6705	0.3726
			0.2			1.0354	2.6849	0.3705	0.9129	0.0527	18.9274
			0.3			0.9875	2.6967	0.3689	0.8771	0.0527	18.9930
3.0	0.2	0.1	0.2	0.1	0.01	1.0355	2.6848	0.3704	1.0397	2.6845	0.3707
				0.4		1.1377	3.2293	0.3079	1.2198	0.0527	18.9527
				0.6		1.2060	3.6325	0.2736	1.3440	0.0526	18.9974
3.0	0.2	0.1	0.2	0.1	0.4	1.0335	2.9106	0.2848	1.0376	2.9103	0.2849
					0.6	1.0325	3.0269	0.2405	1.0000	0.6369	7.5325
					0.8	1.0316	3.1432	0.1961	1.0000	0.8316	4.0208

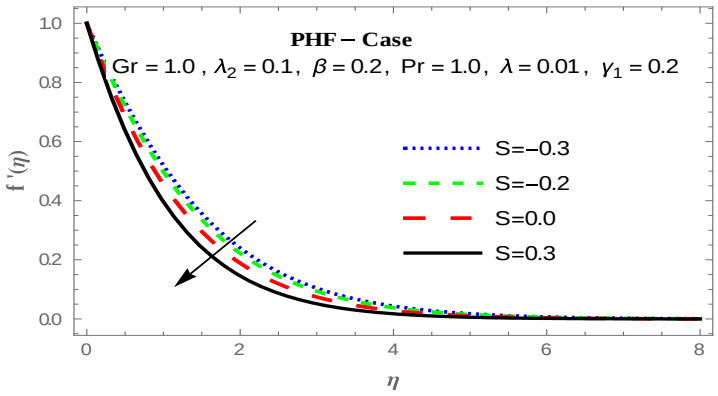

Figure 2: Velocity profiles for varying Suction/Injection parameter S (PHF Case)

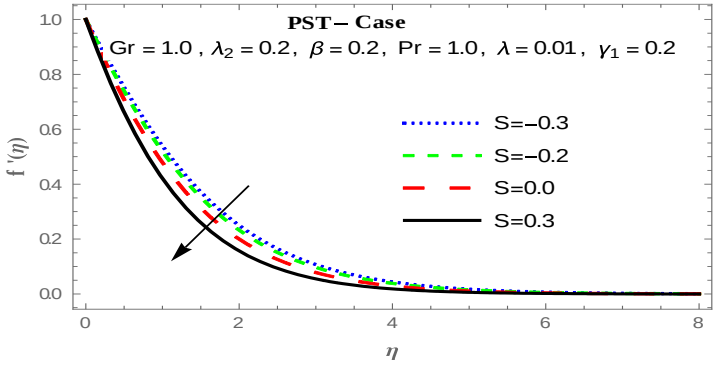

Figure 3: Velocity profiles for varying Suction/injection parameter S (PST Case)

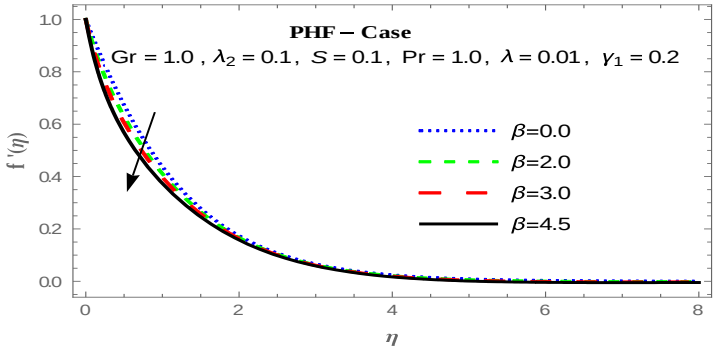

Figure 4: Velocity profiles for varying Ferromagnetic interaction parameter β (PHF Case)

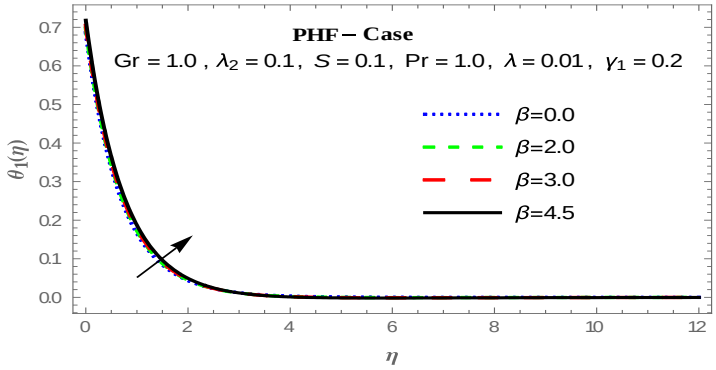

Figure 5: Temperature profiles for varying Ferromagnetic interaction property β (PHF Case)

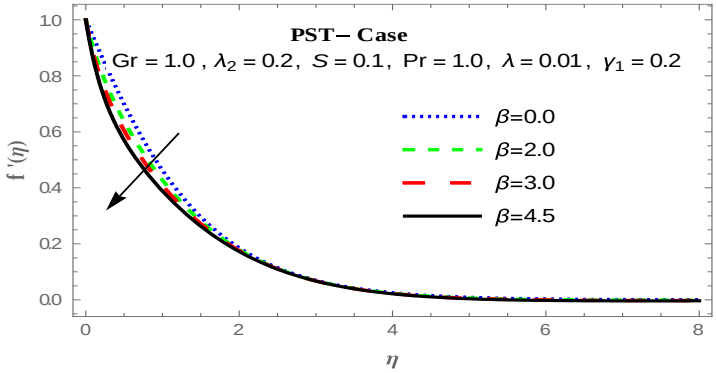

Figure 6: Velocity profiles for varying Ferromagnetic interaction parameter β (PST Case)

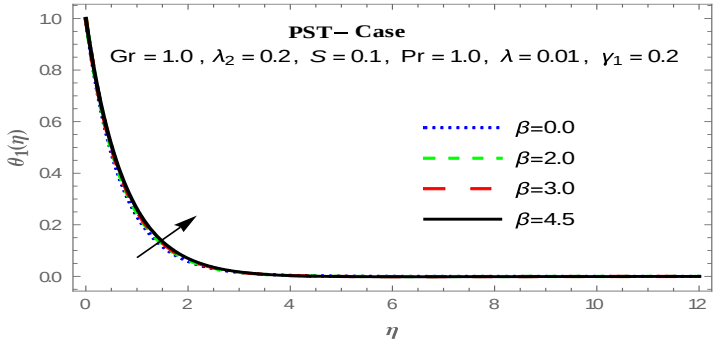

Figure 7: Temperature profiles for varying Ferromagnetic interaction parameter β (PST Case)

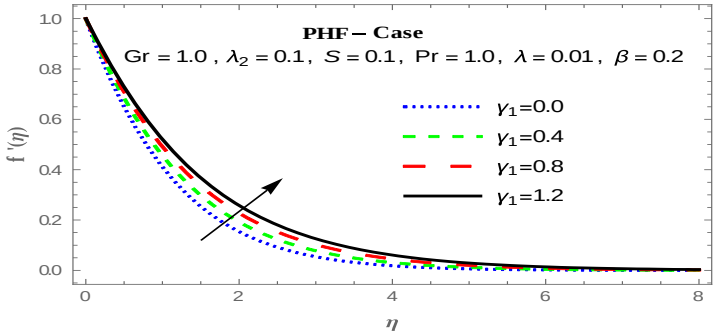

Figure 8: Velocity profiles for varying Deborah number γ_1 (PHF Case)

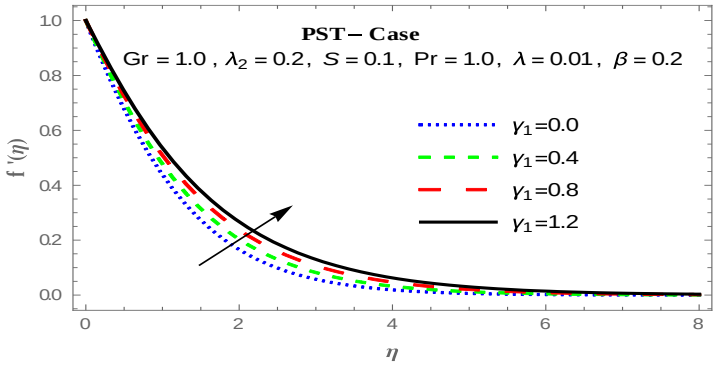

Figure 9: Velocity profile for varying values of the Deborah number γ_1 (PST Case)

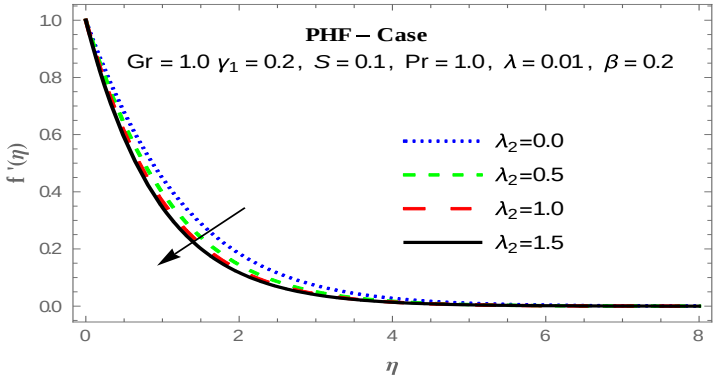

Figure 10: Velocity profiles for varying ratio of relaxation to retardation time λ_2 (PHF Case)

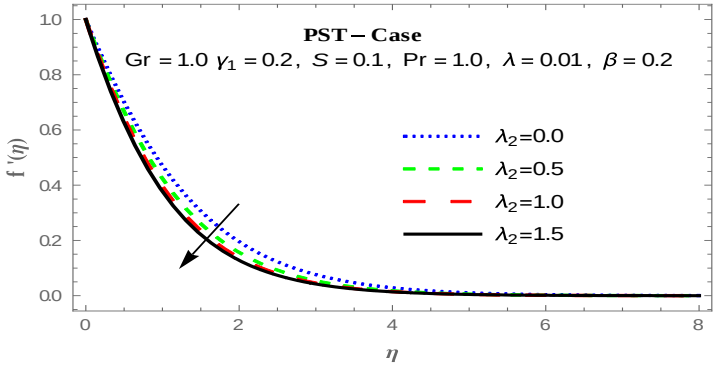

Figure 11: Velocity profiles for varying ratio of relaxation to retardation time λ_2 (PST Case)

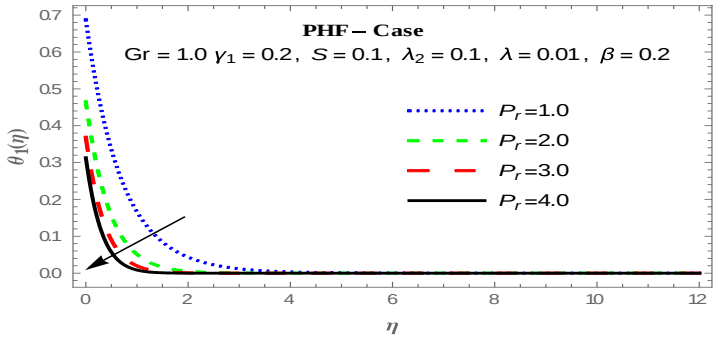

Figure 12: Temperature profiles for varying Prandtl number Pr (PHF Case)

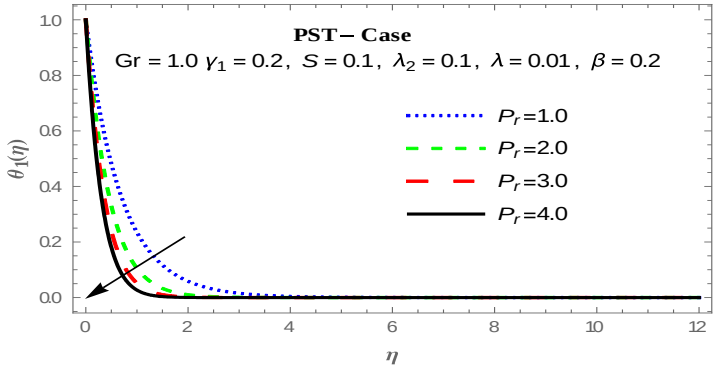

Figure 13: Temperature profiles for varying Prandtl number Pr (PST Case)

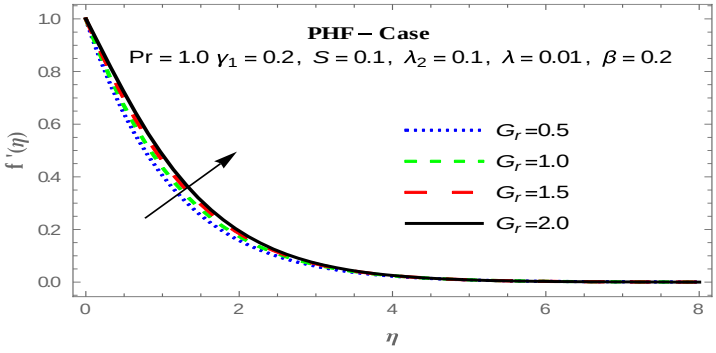

Figure 14: Profile of velocity for varying Grashof number Gr (PHF Case)

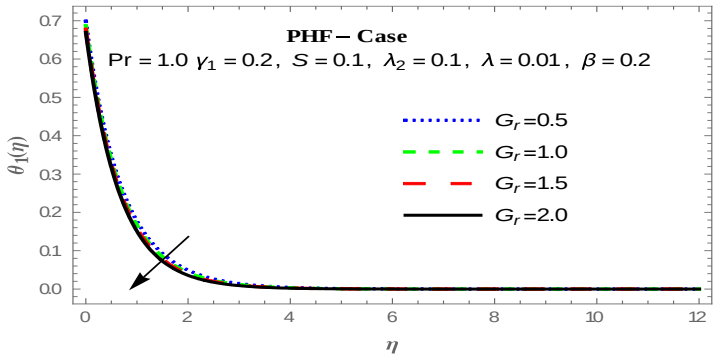

Figure 15: Temperature profiles for varying Grashof number Gr (PHF Case)

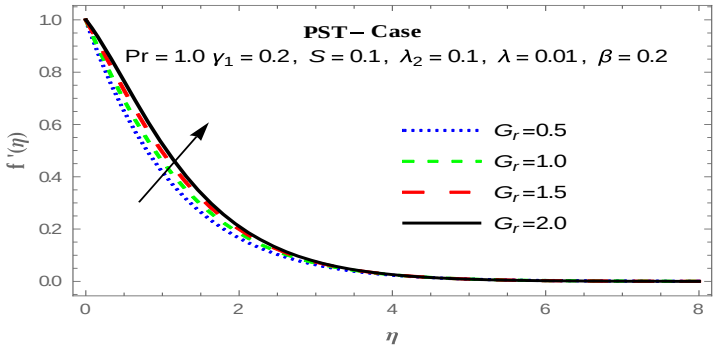

Figure 16: Velocity profiles for varying Grashof number Gr (PST Case)

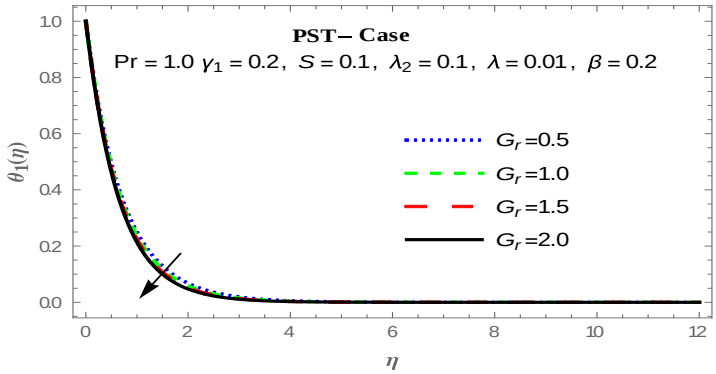

Figure 17: Temperature profiles for varying Grashof number Gr (PST Case)

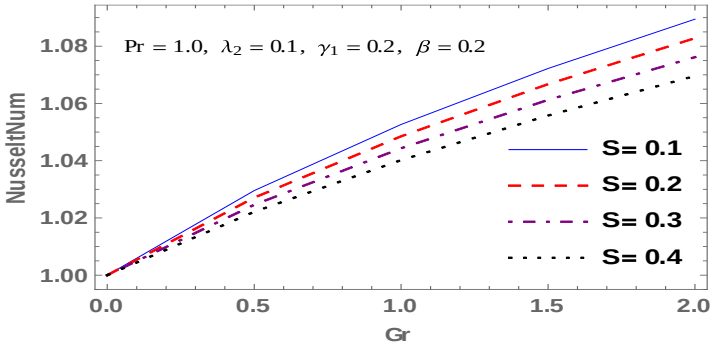

Figure 18: Nusselt number with a variation of Grashof number Gr for various Suction parameter $S > 0$

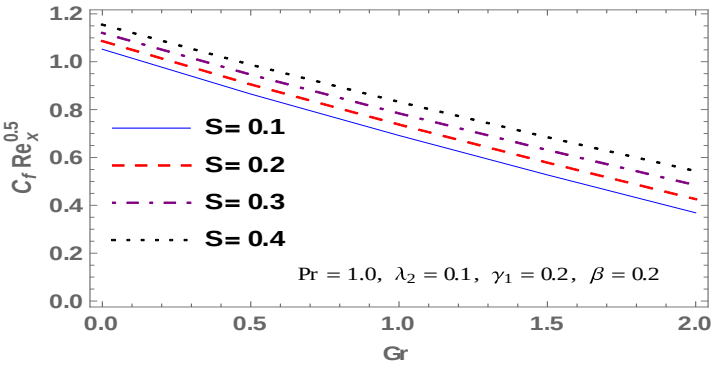

Figure 19: Skin friction coefficient with a variation of Grashof number Gr for various Suction parameter $S > 0$

Table 3: Skin friction coefficient $-f''(0)$ for various values of Pr and Gr with $\beta = 0, 2,\ \lambda = 0.001,\ \lambda_2 = 0.1,\ \gamma_1 = 0.2,\ S = 0.1$.

		$-f''(0)$			
Gr	Pr	PST		PHF	
		$\beta = 0$	$\beta = 2$	$\beta = 0$	$\beta = 2$
1		0.730904	1.238790	0.870781	1.096920
2		0.481351	0.977297	0.752195	1.002500
3	2	0.242750	0.729975	0.638710	0.884691
4		0.012655	0.493060	0.529472	0.771833
5		−0.210488	0.264331	0.423850	0.663123
6		−0.427790	0.042318	0.321374	0.557957
	1	0.316356	0.862192	0.527184	0.888433
	2	0.481351	0.977297	0.752195	1.002500
2	3	0.567310	1.026700	0.835139	0.996929
	4	0.622447	1.019740	0.877407	1.004680
	5	0.661716	1.034330	0.902785	1.007730
	6	0.723047	1.043720	0.919658	1.008900

DISCUSSION

The Chebyshev spectral collocation method (CSCM) was verified for the Nusselt number $-\theta_1'(0)$ at different Prandtl number Pr values and a comparison was done with results from Abel *et al.* [19] as well as Zeeshan and Majeed [1] and presented in Table 1. From the table it can be observed that the results have a good agreement.

Table 2 presents a comparison between results gotten by Chebyshev Spectral Collocation Method (CSCM) and those solutions based on the method in Zeeshan and Majeed [1] for Nusselt number and skin friction coefficient when the Grashof number equals zero. This shows that there is a very good agreement and establishes Chebyshev Spectral Collocation Method (CSCM) as an efficient approach.

In Figure 2, it is shown that fluid velocity reduces throughout the profile as the value of the suction/injection parameter becomes more positive (that is, when $S > 0$), but when $S < 0$ there is an increase in velocity as S becomes less negative. For Figure 3, the velocity tends to reduce throughout the profile as suction/Injection parameter increases ($S > 0$). But when $S < 0$, we see an increase.

Figure 4 indicates that increase in ferromagnetic interaction parameter leads to reduction in velocity of the flow over the plate. Increase in ferromagnetic interaction parameter increases fluid temperature as can be seen in Figure 5, although there is not much difference between the profiles as the values of β increases. β describes the influence of the magnetic force due to the magnetic dipole. Magnetic force delays velocity, hence, when β increases the holdback force also increases, thereby resulting in a reduction of the velocity. Variation of magnetic property causes a divergence of Lorentz force, which results in limitations to the transportation of the fluid. It is also noticed that fluid velocity is more in the absence of magnetic field, that is, when $\beta = 0$ for both PHF and PST processes (Figure 4 and Figure 6). Velocity is reduced, hence there is an increase in frictional heating within the layers of the fluid causing fluid temperature to rise. Figure 7 shows an increase in the temperature as β increases for the prescribed surface temperature case, because the fluid is more viscous and there is a high rate of heat transfer between fluid particles.

Figure 8 reveals that as Deborah number increases, there is corresponding increment in fluid velocity for the prescribed heat flux process. Figure 9 shows that as the Deborah number becomes larger there is increment in fluid velocity for the PST case. Since Deborah number is of direct proportion to the retardation time; when retardation time of a fluid is large it reduces in viscosity, that could lead to increment in the velocity.

Figure 10 depicts that higher values of the ratio of relaxation to retardation time λ_2 leads to decrease in the motion of the fluid. Increasing λ_2 means lower retardation time and higher relaxation time, that is, it takes more time for the rate of flow of the fluid to be enhanced. This also brings about a rise in the temperature of the fluid. For the PST case shown in Figure 11, there is reduction in fluid velocity as ratio of relaxation and retardation time increases.

In Figure 12, Prandtl number increase leads to fall in fluid temperature for the PHF thermal process. Because thermal conductivity of the fluid is quite low for bigger Prandtl number value, and so conduction and thermal boundary layer thickness is reduced. For PST case in Figure 13, there is also a drop in temperature as Prandtl number increases throughout the profile.

Figure 14 shows effect of Grashof number on fluid velocity for the PHF case. As the Grashof number increases, there is an increment in fluid velocity. Figure 15 reveals a fall in fluid temperature as Grashof number increases. As seen in Figure 16, increase in Grashof number for the PST case results in a corresponding increase in the velocity of the fluid. When Grashof number increases in Figure 17, there is a drop in the temperature of the fluid for PST case. The increase in velocity is caused by the gravitational pull exerted on the fluid when the stretching plate is vertically inclined.

As noticed in Figure 18, where Nusselt number is taken as $\dfrac{\theta_1'(0)}{\theta_1'(0)\big|Gr=0}$; As Grashof number increases, the Nusselt number also increases for each value of the suction parameter. As suction parameter increases, Nusselt number profile falls, because higher suction parameter reduces the rate of heat transfer. Figure 19 depicts the behaviour of the skin friction coefficient as Grashof number is varied for various suction parameter values. Increase in Grashof number leads to a fall in skin friction for each value of suction parameter $S > 0$. But, the higher the suction parameter the higher the skin friction coefficient; because higher values of suction parameter reduce the fluid velocity as the frictional force between the fluid and the stretching plate is stronger.

Table 3 shows the skin friction coefficient for various Grashof number Gr values and Prandtl number $\Pr$, considering PST and PHF heating processes when there is no effect of the magnetic dipole ($\beta = 0$) and when there is a magnetic dipole effect ($\beta = 2$). Here, skin friction experience reduction as Grashof number rises and increment as Prandtl number increase. Also, Grashof and Prandtl numbers are increased as magnetic interaction parameter becomes present ($\beta = 2$) as compared to when it was absent ($\beta = 0$). This reveals that the fluid is enhanced with magnetic dipole being present.

CONCLUSION

Following previous work by Zeeshan and Majeed [1], this paper carried out the analysis of Jeffery fluid over vertical stretchable plate with magnetic dipole and suction/injection. Prescribed heat flux (PHF) and prescribed surface temperature (PST) processes are considered. After performing similarity transformation of the governing equations, Chebyshev spectral collocation approach was used to find solution to the non-dimensional equations. Results were compared with those of Zeeshan and Majeed [1] to verify the efficiency of the method used in this work and an excellent agreement was established. Graphs depicting behaviour of velocity and temperature of the Jeffery ferrofluid for various values of existing parameters were presented. The following results were established from this research work:

a. As Grashof number (Gr) increases fluid velocity increases and the temperature is reduced for PHF and PST heating processes.

b. Increment in Prandtl number ($\Pr$) leads to decrease in fluid velocity with a fall in fluid temperature for PHF and PST processes.

c. Ferromagnetic interaction parameter (β) causes reduction in fluid velocity for both PST and PHF cases and temperature rises for PHF and PST cases.

d. The Deborah number (γ_1) enhances velocity of fluid and temperature is reduced for both the PHF and PST cases.

e. Reduction in fluid velocity and increment in temperature occurs as ratio of relaxation to retardation time parameter (λ_2) increases.

f. Suction/injection parameter (S) reduces both temperature and velocity the fluid for both heating processes.

g. Nusselt number becomes higher as Grashof number rises, while increment in suction parameter ($S > 0$) and Prandtl number leads to smaller Nusselt number.

h. Skin friction falls as Grashof number rises, and increases as Prandtl number and Suction parameter ($S > 0$) grow.

REFERENCES

[1] A. Zeeshan, A. Majeed, Heat transfer analysis of Jeffery fluid flow over a stretching sheet with suction/injection and magnetic dipole effect, *Alexandria Engineering Journal, (2016a),* http://dx.doi.org/10.1016/j.aej.2016.06.014

[2] B.C. Sakiadis, Boundary-layer behavior on continuous solid surfaces. I. Boundary-layer equations for two-dimensional and axisymmetric flow, *AIChE J.* 7 (1961) 26–28.

[3] L.J. Crane, Flow past a stretching plate, *Z. Angew. Math. Phys.* 21 (1970) 645–647.

[4] P.S. Gupta, A.S. Gupta, Heat and mass transfer on a stretching sheet with suction or blowing, *Can. J. Chem. Eng*. 55 (1977) 744–746.

[5] N. Dalir, Numerical study of entropy generation for forced convection flow and heat transfer of a Jeffery fluid over a stretching sheet, *Alexandria Engineering Journal, (2016),* http://dx.doi.org/10.1016/j.aej.2014.08.005

[6] T. Hayat, M. Waqas, S.A. Shehzad, A. Alsaedi, MHD stagnation point flow of Jeffery fluid by a radially stretching surface with viscous dissipation and Joule heating, *J. Hyd. Hydromech.*, 63 (2015) 311-317.

[7] N. Sandeep, C. Sulochana, A. Isaac Lare, Stagnation-point flow of a Jeffrey nanofluid over a stretching surface with induced magnetic field and chemical reaction, *Int. J. Eng. Res. Africa*, 20 (2016) 93–111.

[8] T. Hayat, R. Sajjad, S. Asghar, Series solution for MHD channel flow of a Jeffery fluid, *Commun. Nonlinear Sci. Numer. Simul*. 15 (2010) 2400–2406.

[9] M. Narayana, L.R. Titus, A. Abraham, P. Sibanda, Modelling micropolar ferromagnetic fluid flow due to stretching of an elastic sheet, *Afrika Matematika*, 25 (2014) 667–679.

[10] K. Ahmad, A. Ishak, Magnetohydrodynamic (MHD) Jeffery fluid over a stretching vertical surface in a porous medium, *Propulsion and Power Research*. (2017) 1–8, http://dx.doi.org/10.1016/j.jppr.2017.11.007

[11] L.S. Titus, A. Abraham, Ferromagnetic liquid flow due to gravity-aligned stretching of an elastic sheet, *J. Appl. Fluid Mech.* 8 (2015) 591–600.

[12] M.O. Iyoko, B.I. Olajuwon, Differential transform method approach to the study of an MHD flow of a third-grade fluid with Reynolds' model viscosity and Joule heating, *Kathmandu University Journal of Science, Engineering, and Technology*, 15, no. 1 (June 2021) 1-13.

[13] B.J. Akinbo, B.I. Olajuwon, Influence of convective boundary condition on heat and mass transfer in Walters' B fluid over a vertical stretching surface with thermal-diffusion effect, *Journal of Thermal Engineering*, 7 (November 2021a) 1784-1796.

[14] B.J. Akinbo, B.I. Olajuwon, Radiation and thermal-diffusion interaction on stagnation-point flow of Walters' B fluid toward a vertical stretching sheet, *International Communications in Heat and Mass Transfer,* 126 (July 2021b) 105471. DOI:10.1016/j.icheatmasstransfer.2021.105471.

[15] B.J. Akinbo, B.I. Olajuwon, Viscous dissipation effect on magnetohydrodynamics fluid flow over an exponential surface with influence of thermal radiation and thermal diffusion, *European Journal of Computational Mechanics,* 31_5-6 (April 2023) 583-600. doi:10.13052/ejcm2642-2085.31562.

[16] H.I. Andersson, O.A. Valnes, Flow of a heated Ferrofluid over a stretching sheet in the presence of a magnetic dipole, *Acta Mech.* 128 (1998) 39–47.

[17] R.L. Bailey, Lesser known applications of Ferrofluids, *Journal of Magnetism and Magnetic Materials,* 39 (1983) 178-182.

[18] M.O. Iyoko, B.I. Olajuwon, Study on Impact of Magnetic Dipole and Thermal Radiation on Flow/Heat Transfer of Jeffery Fluid over Stretching Sheet with Suction/Injection, *Journal of Advanced Research in Fluid Mechanics and Thermal Sciences*, 104, Issue 1 (April 2023) 65-83.

[19] M.O. Iyoko, B.I. Olajuwon, O. Fagbemiro, M.T. Raji, Jeffrey fluid flow past inclined stretchable sheet with magnetic dipole and suction/injection, *Theoretical and Applied Mechanics*, 51(2) (2024) 93–118. https://doi.org/10.2298/TAM240203006I.

[20] S. Nadeem, N.S. Akbar, Peristaltic flow of a Jeffrey fluid with variable viscosity in an asymmetric channel, *Zeitschrift fu¨ r Naturforschung*, A 64 (2009) 713–722.

[21] T.W. Akaje, B.I. Olajuwon, Effects of inclined magnetic field and slip boundary condition on heat and mass transfer in Casson Nanofluid flow over a stretching sheet, *Sciences & Tech*nology, 5, no 1, (2020) 15–28.

[22] C.D. Pruett, C.L. Streett, A spectral collocation method for compressible, non-similar boundary layers, *International Journal for Numerical Methods in Fluid*, 13 (1991) 713–737.

[23] M.G. Sobamowo, L.O. Jayesimi, M.A. Waheed, Chebyshev spectral collocation method for flow and heat transfer in magnetohydrodynamic dissipative Carreau nanofluid over a stretching sheet with internal heat generation, *AUT Journal of Mechanical Engineering*, 3(1) (2019) 3–14. DOI: 10.22060/ajme.2018.14196.5712

[24] M.S. Abel, E. Sanjayanand, M.M. Nandeppanayar, Viscoelastic MHD flow and heat transfer over a stretching sheet with viscous and ohmic dissipations, *Communications in Nonlinear Science and Numerical Simulation*, 13 (2008) 1808–1821.